High Amplitude, Ultrashort, Longitudinal Strain Solitons in Sapphire

Otto L. Muskens* and Jaap I. Dijkhuis

Atom Optics and Ultrafast Dynamics, Debye Institute, Faculty of Physics and Astronomy, University of Utrecht, P.O. Box 80 000, 3508 TA, Utrecht, The Netherlands

(Received 12 July 2002; published 30 December 2002)

We demonstrate the development of high-amplitude picosecond strain pulses in a sapphire single crystal into an ultrafast compressional soliton train. For this purpose, large-intensity light pulses were used to excite a metal film, yielding a 2 orders of magnitude higher strain than that achieved in earlier studies. Propagation of the packets is monitored over a distance of several millimeters by means of Brillouin light scattering. A one-parameter model, based on the Korteweg–de Vries–Burgers equation, simultaneously explains the observed behavior at all strains and temperatures under study. We predict up to 11 solitons in the train, reaching pressures as high as 40 kbar and 0.5 ps temporal widths.

DOI: 10.1103/PhysRevLett.89.285504 PACS numbers: 63.20.–e, 62.30.+d

In recent years, picosecond longitudinal acoustic pulses have been applied successfully to analyze nanometer-sized structures and thin-film multilayers [1–3]. In a conventional picosecond ultrasonics setup, a minute fraction of the energy of an optical laser pulse (typically 0.1 mJ/cm^2) is converted to a coherent acoustic strain of the order of 10^{-5}, depending on the transducer used. At these low strains nonlinear effects play no role unless the strain pulse is allowed to propagate over long distances.

In a pioneering series of experiments in large crystals at low temperatures, Hao *et al.* [4,5] demonstrated that indeed a propagation distance of millimeters is sufficient to convert a low-strain wave packet into a soliton and an oscillating tail. These results were shown to be consistent with simulations based on the Korteweg–de Vries (KdV) equation in one dimension, signifying that the lattice itself provides sufficient dispersion for soliton development. The combination of high strain values on short length scales sets the stage for a range of striking nonlinear phenomena. Extension to higher strains may lead to solitons over much shorter distances, as well as the generation of extremely fast solitons and soliton trains. Breakup has been demonstrated experimentally of long-wavelength disturbances in water basins and liquid-gas mixtures into soliton trains of considerably higher frequencies [6,7]. Until now, no attempts have been made to find similar phenomena in the field of ultrashort acoustic pulses in solids. Recent experiments have shown atomic motion under high impulsive strain [8–10] and the development of shock waves in metal films [11,12]. However, those experiments focused only on the propagation over micrometer distances, much too short to obtain ultrafast soliton trains.

In this Letter, we demonstrate for the first time the development of high-amplitude strain pulses into a soliton train in sapphire at low temperatures. We increase the strain amplitude of the wave packets in picosecond ultrasonics by 2 orders of magnitude using an amplified ultrafast Ti:sapphire laser system (Spectra Physics "Hurricane"). The output beam of the laser carries 0.75 mJ per pulse at a repetition rate of 1.0 kHz and is lightly focused to a spot of several millimeters in diameter onto the sample. The sample is a sapphire single crystal of $5 \times 11 \times 10$-mm^3 dimensions, with the c axis perpendicular to the 5×11-mm^2 surface. A 1000-Å chromium film is deposited onto this surface. The crystal is mounted into an optical cryostat to perform experiments down to liquid helium temperatures. The optical pump fluence is varied by changing the position of the focusing lens, the upper limit being the damage threshold of our transducer at $\sim$15 mJ/cm^2.

Transient changes of the refractive index due to the presence of the acoustic wave packets are detected by means of Brillouin scattering. Momentum conservation selects a narrow range of Fourier components of the acoustic wave packet. The frequency-shifted optical beam is analyzed with a quintuple-pass Fabry-Pérot interferometer and detected by a gated photon-counting system. This setup has been used recently to observe mode-locked acoustic wave packets [13,14] and coherent, monochromatic phonon beams [15,16]. Acoustic frequency components up to $\sim$30 GHz in sapphire can be studied using the scattering configuration through the side windows of the cryostat (see Fig. 1). Our choice of the metal transducer guarantees an initial wave packet with GHz components [17]. The excellent attachment of

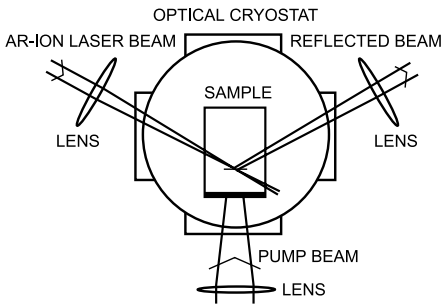

FIG. 1. Top view of the Brillouin scattering configuration in the crystal.

chromium to sapphire and the small acoustic mismatch results in an acoustic reflection coefficient at the interface of only 10%.

Brillouin scattering is the ideal technique to study the development of the wave packet into soliton trains because the propagation distance can be continuously varied and the expected spatial walk-off between the solitons corresponds to wave vectors around the typical scattering wave vector, yielding excellent sensitivity. We have chosen to focus the Brillouin laser tightly to a waist of ~ 4 μm, to achieve an optimal spatial resolution in the propagation direction.

Numerical simulations of the Korteweg–de Vries–Burgers (KdV-Burgers) equation were performed using a discrete, implicit scheme of second order accuracy and three-level quadratic approximation in time [18]. In those cases where solitons were formed, part of the simulation was further evolved using the analytical methods for soliton trains of Ref. [19]. In all calculations, we use the known parameters for the elastic constants of second and third order and the phonon dispersion around the c axis of sapphire [5].

Figure 2 shows typical traces of the acoustic power vs propagation distance at 22 GHz, at room temperature and for six values of the pump fluence. Note the vertical rescaling and horizontal expansion in the figure for the first 0.5 mm propagation distance. At all fluences the Brillouin intensity initially sharply decreases with distance, followed by a weak and slow oscillation. Simulations have been included in the figure using the KdV-Burgers equation. For the viscosity of sapphire at room temperature we took 4.54×10^{-4} Ns/m^2 [20]. Fitted values for the initial acoustic strain s_0, the single adjustable parameter of the model (except for the overall amplitude), are presented as numbers in Fig. 2(c). Good agreement between theoretical and experimental traces is obtained for values of s_0 around 10^{-3}, which corresponds to a transient pressure of 10 kbar. These values coincide with the absolute Brillouin intensity, gauged against the measured thermal phonon background in the absence of strain pulses. Further, temporal traces obtained from the simulation after a 5-mm propagation distance are included in Fig. 2(c), which exhibit the typical shape of the damped N-wave solution of the Burgers equation [21]. From these simulations we conclude that, at room temperature, the degree of self-steepening does not reach the critical value in order to bring dispersion into play.

The propagation at intermediate temperatures is shown in Fig. 3 and shows the typical crossover from overdamped to virtually undamped propagation. Again, simulations have been performed succesfully, by taking a linear temperature dependence of the viscosity above 100 K [16]. This makes our simulation adjustable parameter-free. The onset of fast oscillations in the propagation, between 50 and 100 K, signifies the formation of solitons, as we show in the following section.

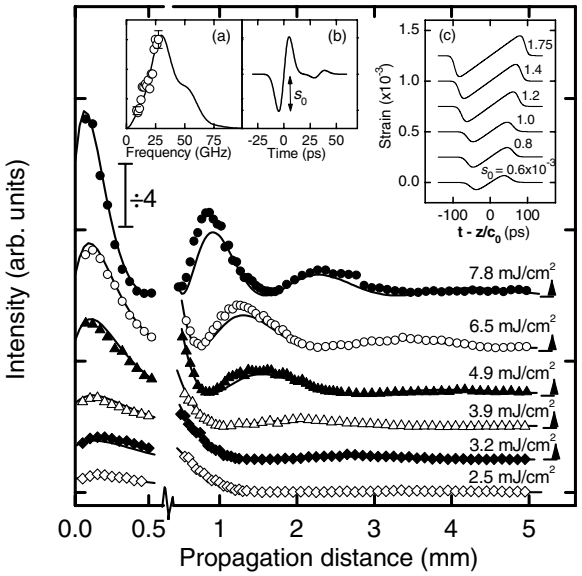

FIG. 2. Acoustic power at 22 GHz as a function of propagation distance in the sapphire crystal, at room temperature. Points: experimental data. Lines: numerical simulations. Arrows indicate vertical offsets. Up to 0.5 mm, traces have been vertically divided by 4. Inset (a): power spectrum of the initial wave packet used in simulations, with Brillouin intensity (points) obtained at different scattering angles. (b) Initial waveform used in simulations. (c) Time-domain waveforms after 5 mm of propagation, in the moving-frame coordinate $t - z/c_0$, obtained from simulations with corresponding values of acoustic strain s_0.

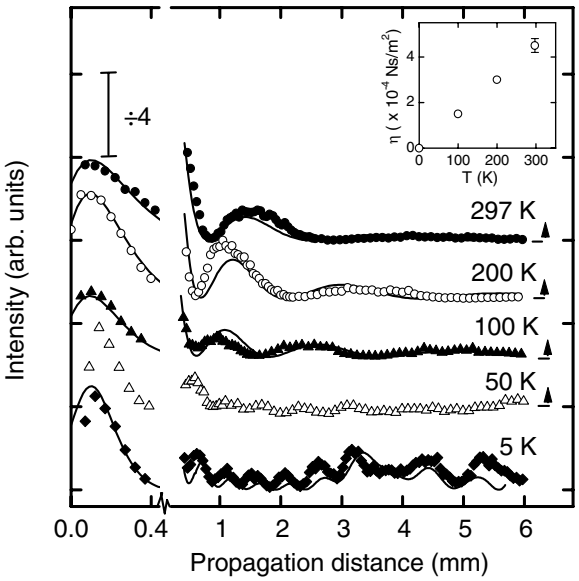

FIG. 3. Traces of the 22 GHz frequency component for different temperatures, at a pump fluence of 4.9 mJ/cm^2. Points: experimental data. Lines: simulations based on the KdV-Burgers equation. Inset: values for the viscosity η used in the simulations.

Simulations in the crossover regime have not been performed, because the specific anharmonic process involved in the damping is not known. At a temperature of 5 K, however, we may neglect damping completely.

Finally, we present traces taken at a temperature of 5 K, again at 22 GHz, and for a range of pump fluences [see Fig. 4(a)]. We observe for all curves an initial decay reminiscent of the behavior at higher temperatures, but slightly faster. Beyond a propagation distance of a few hundred micrometers, we can discern fast oscillations in the acoustic power, with a period decreasing with increasing pump fluence. After a propagation length of several millimeters, the characteristic oscillations become less distinct.

At this point we show that this behavior can readily be simulated by the KdV equation. In the present simulations, proper corrections were made for the strain values to account for the temperature-dependent absorption changes in the transducer [see Fig. 4(b)], leaving us again without any adjustable parameters. The results are plotted in Fig. 4(a) and show a remarkable agreement up to several millimeters propagation length. General features such as the initial decay, fast oscillations, and the transition from an oscillatory to a more complex behavior after several millimeters are correctly reproduced by the calculations.

Figure 4(c) shows the simulated successive stages of the development of the wave packet into a soliton train. Inspection of the experimental data and the simulations reveals that the initial decay of the Brillouin intensity is produced by self-steepening of the wave packet and concomitant up-conversion of the acoustic energy to frequencies as high as 1 THz, i.e., beyond the experimental window. Only at these high frequencies, phonon dispersion provides enough phase accumulation to balance self-steepening and initiate soliton formation in the leading part and the so-called radiative tail in the trailing part. The variations of the Brillouin intensity vs propagation distance can then indeed be traced back to Bragg scattering off the soliton train, with resonance length $\tau_{\mathrm{res}} = 1/\nu_{\mathrm{B}}$ as indicated in the figure (ν_{B} denotes the Brillouin frequency). Two solitons of different amplitudes and consequently different velocities v_1, v_2 would already result in one oscillation, with a period of $\lambda = c_0^2/(v_1 - v_2)\nu_{\mathrm{B}}$, c_0 being the sound velocity. For a velocity difference of $10^{-3}c_0$, this will give an oscillation with a period of $\lambda = 0.51$ mm. N solitons produce $(N-1)!$ spatial resonances at maximum, resulting in a complicated beating pattern as a function of propagation distance, as we observe experimentally. We examine in Fig. 4(d) the spatial-Fourier transform of one of the experimentally obtained diagrams of Fig. 4(a) and resolve at least nine distinct contributing frequencies. This directly poses a lower limit on the number of solitons (and tail) of $N = 5$. From the simulation it can further be observed that the distances between the solitons are almost equal, implying degeneracy of many spatial resonances and a reduction of the number of experimentally observable beating frequencies. The limited propagation length in our experiments unfortunately prevents an exact determination of the number of solitons in the train directly from the spatial-Fourier spectrum of Fig. 4(d). However, accurate knowledge of all material parameters and experimental conditions allows us to define a prototype wave packet, the soliton train of Fig. 4(c), that is consistent with all our experimental data.

The bold extrapolation from the GHz Brillouin-scattering data to the THz characteristics of the wave packet is in our opinion justified by the excellent agreement between the experimental and computed behavior.

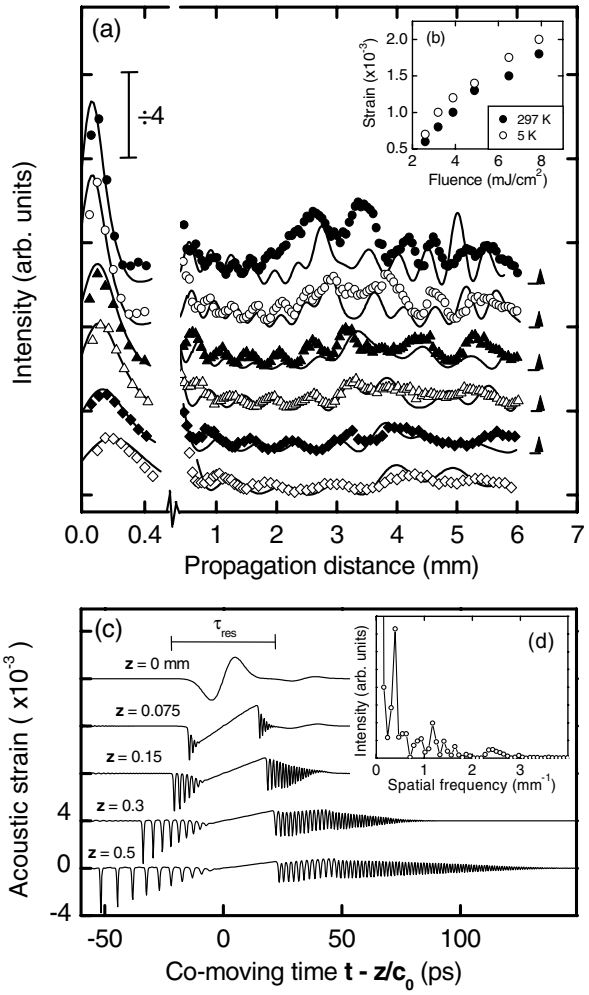

FIG. 4. (a) Scans of the 22 GHz Fourier component of the acoustic wave packet, for different pump fluences, at a temperature of 5 K. Points: experimental data. Lines: simulations based on the KdV equation. (b) Values for the acoustic strain obtained for the simulations at temperatures of 293 and 5 K. (c) Time domain traces, for several propagation distances z, obtained from simulations based on the KdV equation, for an initial strain of 1.75×10^{-3}. (d) Fourier transform of the experimental scan of (a) at 6.5 mJ/cm^2.

In the problem of nonlinear wave propagation, one cannot simply separate the behavior of the high- and low-frequency components of the wave packet: they are inherently coupled and interlaced. This fact allows one to draw detailed conclusions on the evolution of high-frequency components, once the low-frequency behavior is assessed to sufficient precision as we did using Brillouin spectroscopy. A viscously damped N wave must evolve according to a typical diffusive scaling law [21], which explains the slowing down of the oscillations in the high-temperature Brillouin data. KdV solitons propagate with constant velocity and therefore will exhibit a constant oscillation period in the Brillouin signal. As the KdV soliton is a one-parameter entity, its amplitude and width follow directly from this velocity. Inelastic light scattering thus forms a unique monitor of soliton-train evolution inside a crystal, despite the fact that the solitons consist of very high-frequency components, far beyond the bandwidth of a Brillouin spectrometer.

In conclusion, we have efficiently generated planar, high-intensity acoustic wave packets of picosecond duration and monitored their propagation using Brillouin scattering. High-intensity optical excitation yields a 2 orders of magnitude higher strain and correspondingly higher conversion of absorbed energy to coherent phonons than conventional picosecond ultrasonics. Experiments at low temperature have been described successfully by the KdV equation. From these calculations, we predict the development of an acoustic soliton train of up to 11 individual solitons, reaching a strain as high as 4×10^{-3}, a subpicosecond time duration, and a 5-nm spatial width. Further measurements show that solitons can be formed at temperatures as high as 50 K. Above 100 K, damping of high acoustic frequencies completely eliminates the role of dispersion, resulting in weak shock wave formation.

Potential applications of intense subpicosecond acoustic pulses are in strain-induced chemistry and surface science, and possibly switching of synchrotron beams [22,23]. Further, the small acoustic wavelength and highly localized energy content make ultrashort acoustic solitons a potentially suitable vehicle for patterning or imaging of nanometer-scaled objects. The feasibility to generate these pulses up to liquid nitrogen temperatures may therefore be of technological relevance. Research at even higher nondestructive excitation intensities will be possible but requires a stronger or embedded transducer. Intense subpicosecond acoustic wave packets will certainly open up new areas of fundamental research on vibrational dynamics [24] and phonon localization in glasses [25,26]. Finally, the single-cycle pulse shape and quadratic nonlinearity provide a new and fascinating playground for fundamental studies on one- and higher-dimensional solitons, in analogy with their optical counterparts [27,28].

The authors thank P. Jurrius, C. R. de Kok, and F. J. M. Wollenberg for their technical assistance. This work was supported by The Netherlands Foundation "Fundamenteel Onderzoek der Materie (FOM)" and the "Nederlandse Organisatie voor Wetenschappelijk Onderzoek (NWO)."

*Electronic address: O.L.Muskens@phys.uu.nl

[1] O. B. Wright, B. Perrin, O. Matsuda, and V. E. Gusev, Phys. Rev. B **64**, 081202 (2001).
[2] K. E. O'Hara, X. Hu, and D. Cahill, J. Appl. Phys. **90**, 4852 (2001).
[3] M. Nikoonahad, S. Lee, and H. Wang, Appl. Phys. Lett. **76**, 514 (2000).
[4] H.-Y. Hao and H. J. Maris, Phys. Rev. Lett. **84**, 5556 (2000).
[5] H.-Y. Hao and H. J. Maris, Phys. Rev. B **64**, 064302 (2001).
[6] D. A. Horn, J. Imberger, and G. N. Ivey, J. Fluid Mech. **434**, 181 (2001).
[7] V. V. Kuznetsov, V. E. Nakoryakov, B. G. Pokusaev, and I. R. Schreiber, J. Fluid Mech. **85**, 85 (1978).
[8] D. A. Reis *et al.*, Phys. Rev. Lett. **86**, 3072 (2001).
[9] A. Cavalleri *et al.*, Phys. Rev. Lett. **85**, 586 (2000).
[10] C. Rose-Petruck *et al.*, Nature (London) **398**, 310 (1999).
[11] K. T. Gahagan *et al.*, Phys. Rev. Lett. **85**, 3205 (2000).
[12] R. Evans *et al.*, Phys. Rev. Lett. **77**, 3359 (1996).
[13] O. L. Muskens and J. I. Dijkhuis, Physica (Amsterdam) **316B–317B**, 373 (2002).
[14] O. L. Muskens and J. I. Dijkhuis, in "Proceedings of Optical Solitons: Theory and Experiments, 2002" (Springer-Verlag, Berlin, to be published).
[15] E. P. N. Damen, D. J. Dieleman, A. F. M. Arts, and H. W. de Wijn, Phys. Rev. B **64**, 174303 (2001).
[16] E. P. N. Damen, A. F. M. Arts, and H. W. de Wijn, Phys. Rev. B **59**, 349 (1999).
[17] O. B. Wright and K. Kawashima, Phys. Rev. Lett. **69**, 1668 (1992).
[18] J. H. Ferziger and M. Perić, *Computational Methods for Fluid Dynamics* (Springer-Verlag, Berlin, 1999), 2nd ed.
[19] V. I. Karpman, *Non-Linear Waves in Dispersive Media* (Pergamon Press, Oxford, 1975), 1st ed.
[20] B. A. Auld, *Acoustic Fields and Waves in Solids* (Robert E. Krieger Publishing Company, Malabar, FL, 1990), 2nd ed.
[21] G. B. Whitham, *Linear and Nonlinear Waves* (Wiley, New York, 1974), 1st ed.
[22] M. F. DeCamp *et al.*, Nature (London) **413**, 825 (2001).
[23] A. Cavelleri *et al.*, Phys. Rev. Lett. **87**, 237401 (2001).
[24] J.-P. R. Wells, R. E. I. Schropp, L. F. G. van der Meer, and J. I. Dijkhuis, Phys. Rev. Lett. **89**, 125504 (2002).
[25] B. Hehlen *et al.*, Phys. Rev. Lett. **84**, 5355 (2000).
[26] Ts. Nakayama, Phys. Rev. Lett. **80**, 1244 (1998).
[27] X. Liu, K. Beckwitt, and F. Wise, Phys. Rev. E **62**, 1328 (2000).
[28] W. E. Torruelas *et al.*, Phys. Rev. Lett. **74**, 5036 (1995).